Investigation of the thermal performance of cascaded latent heat thermal energy storage system based on composite phase change materials

Investigation of thermal performance of cascade latent heat thermal energy storage system based on composite phase change materials

Qunli Zhang[a], Yimo Liu[a], Zhaosheng Yang[a], Gang Wang[a], Xiaoshu Lü[b,c]

[a]Beijing Municipality Key Lab of Heating, Gas Supply, Ventilating and Air Conditioning Engineering, Beijing University of Civil Engineering and Architecture, Beijing, 100044, P.R. China

[b]Department of Electrical Engineering and Energy Technology, University of Vaasa, P.O.Box 700, FIN-65101, Vaasa, Finland

[c]Department of Civil Engineering, Aalto University, P.O.Box 12100, FIN-02130, Espoo, Finland

Abstract: This paper conducts thermodynamic analysis of the cascaded latent heat thermal energy storage system (C-LHTESS) that is applicable to building heat storage system with a foucs on improving performance of sift non-toxic composite phase change materials. In addition, the technical advantages of using such materials in C-LHTESS heat transfer enhancement systems in heat utilization still need to be studied and analyzed. This paper solved the above problems to provide theoretical guidance of the C-LHTESS into building heat storage equipment. In order to obtain the non-toxic phase change materials, MgSO4 • 7H2O-KAl(SO4)2 • 12H2O , stearic acid, and 60# paraffin was screened and the C-LHTESS with these materials was put forward. Multiple evaluation index were used to compare the C-LHTESS system with the single-stage system from different perspectives. The results show that the non-toxic composite materials used in C-LHTESS can significantly improve the heat charge and discharge efficiency, and the thermal recovery efficiency of the system is optimized. Finally, the influence of the flow state of the heat transfer fluid in the C-LHTESS on heat charging efficiency is analyzed. It is found that increasing a large amount of flow velocity only brings a small increase in heat transfer efficiency when Reynolds number is large. From the perspective of reducing energy consumption, it is recommended that the Reynolds number of the heat transfer fluid is about 2000 and the flow state is laminar.

Keywords: Phase change material, Heat transfer enhancement, Thermal storage, Numerical simulation

Highlights:

- **A low temperature C-LHTESS with non-toxic phase change material was put forward.**
- **Transient thermal model of C-LHTESS is developed and validated.**
- **Multiple evaluation index were used to evaluate the system from different perspectives.**
- **The influence of system structure and flow state of heat transfer fluid on performance was studied and ansysed.**

1. Introduction

The global energy transition is under way with more diversified fuels as a result of the coming low-carbon future, and energy demand is switching to renewables[1-3]. Renewable energy is expected to be the largest energy source in the next 30 years, with wind and solar leading the way, accounting for 60% of primary energy in 2050[4]. So far, the main constraints to the use of renewables are intermittency and volatility[5]. To ensure stable utilization of renewable energy, energy storage is the key, which includes thermal energy and other technologies.

Among thermal energy storage technologies, including sensible, latent and thermochemical heat storages, latent heat thermal energy storage system (LHTESS) presents one of the most effective methods[6, 7]. LHTESS uses phase change materials (PCMs) to charge or discharge latent heat and store it during the phase change process[8]. Because LHTESS has uniform charging and discharging temperature and higher heat storage density, it has more

potentials than sensible heat storage system[9]. Although lots of LHTESS have been developed and applied currently, such as industrial waste heat recovery[10], solar distillation[11], and building air conditioning devices[12], there are still many possibilities for technological improvements of LHTESS[13, 14]. One of the foremost promising ways to enhance LHTESS is to use a cascade heat storage system [15], as shown in Fig.1.

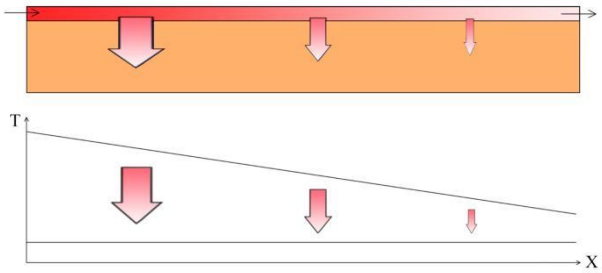

Fig.1-1. Conventional latent heat thermal energy storage system

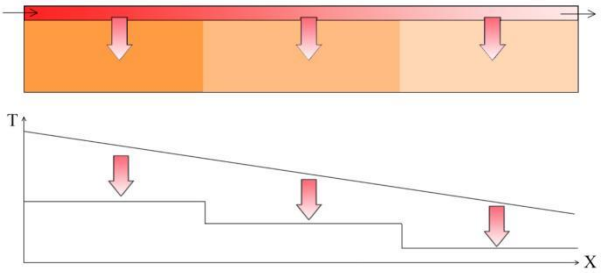

Fig.1-1. Cascade latent heat thermal energy storage system

In the LHTESS, heat exchange between the heat transfer fluid (HTF) and the PCM occurs continuously during the charging and discharging process, where the temperature of the HTF drops steadily along the flow path during the charging phase, and rises steadily during the discharging phase. However, the temperature of the PCM can only stable at the phase change temperature, it eventually reduces the temperature difference between the HTF and the PCM. The decrease in temperature difference results in a reduction in heat flux and heat transfer efficiency, thus decreasing charging and discharging efficiency[16]. The LHTESS with multiple PCMs (cascade system) configures multiple phase change materials in different phase change temperatures along a vertical or fluid flow direction. This ensures that the temperature difference between the HTF and the PCM is nearly constant, thus increasing the average temperature difference[17, 18]. The LHTESS with cascade system has higher heat exchange efficiency and higher exergy efficiencies over the single-stage PCM systems[19-21].

To verify the superiority of the LHTESS with cascade system, the cascade and single-stage systems were compared and analyzed. PEIRÓ et al.[22] designed a LHTESS with phase change temperature about 150-200℃, and found that effectiveness was enhanced by 19.36% with the multiple PCMs configuration system than that with the single PCM system. Dzikevics et al. [23]proposed a mathematical model to evaluate the effects of the PCM in a fully mixed water accumulation tank and compared a single type of PCM and multiple types of PCM systems. The multiple PCMs configuration systems showed lower return temperatures and higher heat storage capacity than the single PCM systems. Yang et al. [24] studied a latent heat storage system using spherical capsules filled with differents kind of PCMs and compared them with a single PCM system. Higher energy and exergy transfer efficiencies were obtained for this advanced latent heat storage system. Bains et al. [25] applied three different PCMs in one heat storage system to investigate the system performance. The study demonstrated that as the flow velocity increases from 2 L/min to 6 L/min, the system charging period is reduced by 28% to 14%. And as the mass flow rate increases, the energy storage efficiency increases but the exergy efficiency decreases. Aldoss et al. [26] studied the number of stages in the cascade heat storage system. They discovered that the three stages approach the linear reference case without the need for additional stages.

The literature review has clearly shown that the the LHTESS with cascade system under the suitable conditions performs better than traditional systems. Although there have been extensive research on LHTESS, there are few studies of non-toxic materials used in heat storage systems. As more heat storage devices are being used in buildings, such as phase change heat storage water tank andphase change heat storage radiator, it is very important to control the toxic effect of PCMs on indoor environment. Therefore, it is necessary to sift non-toxic phase change materials in design. Chandel et al.[27] reviews the toxicity and health hazards of PCMs and. Such a toxic issue has not been paid attention to in previous studies. Many PCMs may be harmful to human health. Therefore, one of the aims of this study was to develop an alternative non-toxic PCMs in the system to reduce the advserse impacts on human health. This

paper fills the research gap in the literature by investigating the cascade LHTESS based on non-toxic materials that is applicable to building heat storage equipment. Three kinds of PCMs were selected with phase transition temperatures of 80℃, 70℃ and 60℃, respectively[28]. It was found that Ba(OH)2 • 8H2O, stearic acid and 60# paraffin are suitable for phase transition temperature with many practical applications[29-31]. However, the Ba(OH)2 • 8H2O aqueous solution is strongly alkaline, and the barium ions can cause serious damage to the respiratory, nervous and digestive systems. Here, we propose a new composite PCM to replace Ba(OH)2 • 8H2O and aim to modify it to improve its thermal conductivity.

The process of heat charging and discharging in the cascade LHTESS with composite PCM was investigated and its performance was compared to the single-stage LHTESS with different PCMs. The advantages of the cascade heat storage system wereexplored. The main goal of this study is to provide more information on optimal design of low temperature heat storage systems.

2. Materials and methodology

2.1 The PCM performance

In the practical application process, the requirements of thermal properties, crystal dynamics, safety, and economy should be met for a relatively ideal PCM.

On the basis of meeting these requirements, many scholars have done a lot of work on the different combinations of PCM in LHTESS. In order to obtain the cascade LHTESS suitable for district heating system, three kinds of PCM with phase change temperatures of 80°C, 70°C and 60°C were selected. Ba(OH)2·8H2O, stearic acid and 60# paraffin are the materials with high latent heat and suitable phase change temperature. Since Ba(OH)2·8H2O has certain damage to human body, this paper uses MgSO4·7H2O-KAl(SO4)2·12H2O binary PCM to replace Ba(OH)2·8H2O. Through experiments, it is found that the supercooling degree of MgSO4·7H2O material itself is not high.After the addition of KAl(SO4)2·12H2O, the undercooling degree of the binary PCM is increased, which is mainly due to the high undercooling degree of KAl(SO4)2·12H2O, so it needs to be modified.

The method to reduce the degree of undercooling is to add nucleating agent to PCM, whose main role is to act as the crystal nucleus needed for crystallization of PCM in the molten state, thus speeding up the crystallization speed during solidification. And the way to improve the thermal conductivity is to add thermal conductivity enhanced filler into the PCM.Expanded graphite is one of the common thermal conductivity enhancement materials. After adding expanded graphite into PCM, it can also be used as the crystal nucleus of PCM crystallization, and can also reduce the degree of undercooling of PCM to a certain extent.

In this paper, melt impregnation method was selected as the composite method to prepare EG-PCM composite phase change material, and the DSC test results are shown in the Fig.2. Compared with pure MgSO4·7H2O-KAl(SO4)2·12H2O binary PCM, the latent heat of EG-PCM composite phase change material decreased by 5.54%. It can be seen that the latent heat of EG-PCM composite PCM decreased less, and had less influence on phase change temperature.

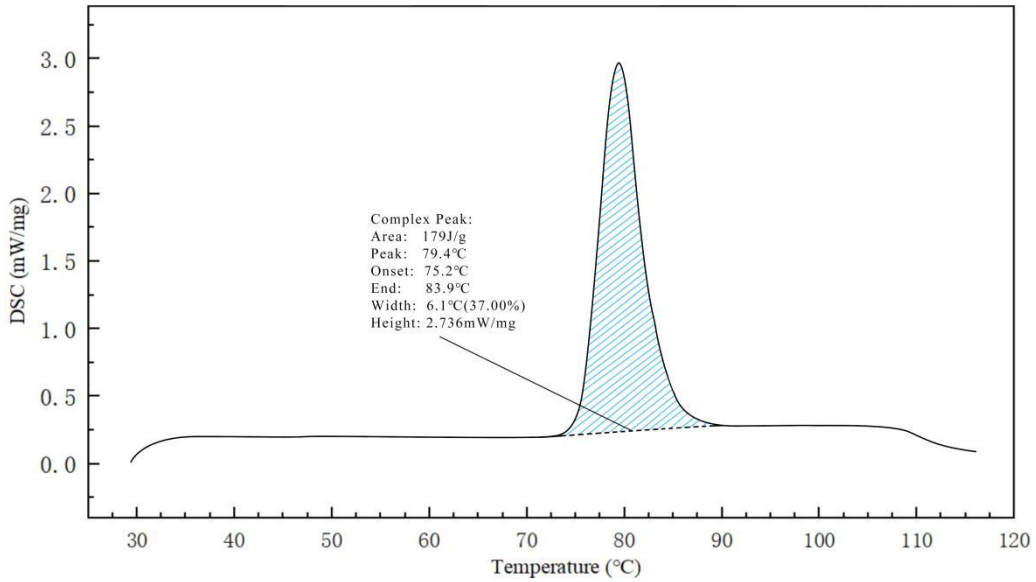

Fig.2. DSC test results of the EG-MgSO4·7H2O-KAl(SO4)2·12H2O

In order to determine the mixing ratio of MgSO4·7H2O-KAl(SO4)2·12H2O and EG, the phase characteristics of dissolved CPCM in 0%EG, 2.5%EG, 5%EG, 7.5%EG and 10%EG were compared[32, 33].The results show that the addition of EG can effectively improve the thermal conductivity of MgSO4·7H2O-KAl(SO4)2·12H2O composite phase change materials.With the gradual increase of EG mass fraction, the thermal conductivity of CPCM system gradually increased, but the lifting effect gradually slowed down.In addition, MgSO4·7H2O - KAl(SO4)2·12H2O binary phase change materials cannot be completely adsorbed into EG when EG mass fraction is 2.5% and 5%.CPCM containing 10wt.%EG reduced latent heat more than CPCM containing 7.5wt.%.Therefore, the eg-MgSO4 ·7H2O-KAl(SO4)2·12H2O composite phase change material prepared by melt impregnation method was selected as the first stage of the cascade phase change regenerator.Stearic acid and 60# paraffin are still used as phase change materials in the second and third stages of the cascade phase change regenerator[34, 35].

Therefore, $MgSO_4 \cdot 7H_2O$-$KAl(SO_4)_2 \cdot 12H_2O$ binary PCM, stearic acid, and 60# paraffin were selected as phase change materials in the cascade heat storage system. These three kinds of PCMs have the advantages of economy, safety, reliability, which are basically meet the requirements. The physical parameters of PCM are shown in Table 1.

Table 1. Physical properties of phase change materials[36]

	Binary phase change material	stearic acid	60 # paraffin	units
melting temperature	79.4	69	61.3	℃
latent heat	175.8	203	206	$kJ \cdot kg^{-1}$
density	1731	941	837	$kg \cdot m^{-3}$
Thermal conductivity	2.53	0.29(s)/ 0.17(l)	0.56(s) /0.36(l)	$W \cdot (m \cdot K)^{-1}$
Specific heat	1.56	1.76(s)/ 2.27(l)	3.20(s)/ 2.8(l)	$kJ \cdot (kg \cdot K)^{-1}$

2.2 Physical model description

Phase-change heat accumulators are mainly shell and tube heat exchangers with many heat transfer tube bundles and baffles inside in practical engineering[37].The purpose of this paper is to present the general law, from the shell

and tube heat exchanger to take a heat transfer unit as the research object, using a simplified casing model as demonstrated in Figure 3-1.

The heat exchanger's overall length (L) is 900mm; the inner tube diameter (2R) is 10mm; and the heat transfer fluid is water. The outer tube diameter (2R) is 50mm; the tubes are connected in a three-stage design, each stage length (L) is 300mm, and binary phase change material, stearic acid, and 60 # paraffin are filled, respectively. The melting temperature of the three groups of materials decreased in turn. The shell is 1mm thick and made of aluminum. The three-dimensional model above is simplified into a two-dimensional axisymmetric model to ensure the rapidity and accuracy of numerical calculation. It was shown in Figure 3-2.

In order to simulate numerically; some assumptions were used as follows:

- Flow was assumed transient and two-dimensional
- The PCM at all levels is evenly distributed and isotropic.
- The thermal conductivity, specific heat, density, and viscosity of PCM are constant at all stages, ignoring the volume change during the phase transformation process.
- The convection effect after PCM melting is ignored.
- The shell wall of LHTESS is adiabatic, ignoring the thermal contact resistance at all levels.
- At starting, temperature of the C-LHTESS was assumed uniform.

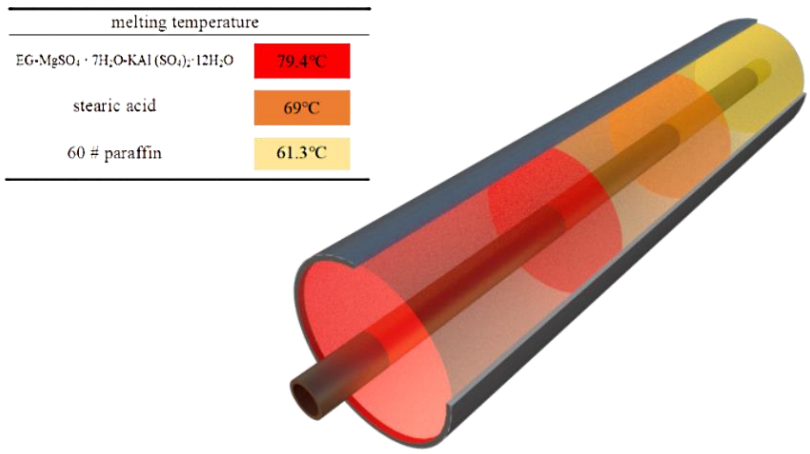

Fig.3-1. Schematic of cascade LHTESS

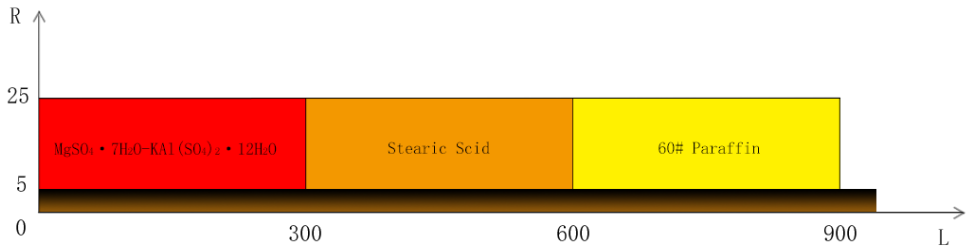

Fig.3-2. Simplified model of the heat storage unit

2.3 Mathematical model description

The governing equations for HTF and PCM are shown in Table 2.

Table 2. The governing equations for HTF and PCM

	Type	Mathematical model	Definition
HTF	Continuity equation	$\frac{\partial v_x}{\partial x}+\frac{\partial v_y}{\partial y}=0$	v_x velocity in the x direction v_y velocity in the y direction

	Momentum equation	$\frac{\partial(\rho_f v_x)}{\partial \tau}+\frac{\partial(\rho_f v_x^2)}{\partial x}+\frac{\partial(\rho_f v_x v_y)}{\partial y}=\mu_f\frac{\partial^2 x}{\partial x^2}+\mu_f\frac{\partial^2 x}{\partial y^2}-\frac{\partial P}{\partial x}$	μ_f dynamic viscosity of the HTF
		$\frac{\partial(\rho_f v_y)}{\partial \tau}+\frac{\partial(\rho_f v_y^2)}{\partial y}+\frac{\partial(\rho_f v_x v_y)}{\partial x}=\mu_f\frac{\partial^2 y}{\partial x^2}+\mu_f\frac{\partial^2 y}{\partial y^2}-\frac{\partial P}{\partial y}$	ρ_f density of the HTF
			c_f specific heat of the HTF
			T_f temperature of the HTF
	Energy equation	$\rho_f c_f\frac{\partial T_f}{\partial \tau}+\rho_f c_f\frac{\partial(v_x T_f)}{\partial x}+\rho_f c_f\frac{\partial(v_y T_f)}{\partial x}=k_f\left(\frac{\partial^2 T_f}{\partial x^2}+\frac{\partial^2 T_f}{\partial y^2}\right)$	k_f thermal conductivity of the HTF
PCM	Energy equation	$\frac{\partial(\rho H)}{\partial \tau}=\nabla\bullet(\lambda\nabla T_p)$ $H=h+(h_l-h_s)$	ρ density of the PCM
			C_p specific heat of the PCM
		$h=h_r+\int_{T_r}^{T_p}C_p dT_p$	β melt fraction of the PCM
		$(h_l-h_s)=\beta L$	λ thermal conductivity of the PCM
			H enthalpy of the PCM
	Melt fraction	$\beta=\begin{cases}0 & T_p<T_s\\ \frac{(T_p-T_s)}{(T_l-T_s)} & T_s<T_p<T_l\\ 1 & T_l<T_p\end{cases}$	h sensible enthalpy of the PCM
			h_l liquid phase enthalpy of the PCM
			h_s solid phase enthalpy of the PCM
			h_r reference enthalpy of the PCM
			T_s solidification temperature of the PCM
			T_l melting temperature of the PCM
			T_p temperature of the PCM

The initial and boundary conditions of the simulation are shown in Table 3.

The HTF flows in from the tubes corresponding to the PCM with a high melting temperature and out from the tubes corresponding to the PCM with a low melting temperature during the charging process. The initial temperature field of each phase change heat storage device was set at 310 K.The inlet temperature of the heat transfer fluid was set at 367 K, and the inlet velocity was 0.2 m/s.

The HTF flows in from the tubes corresponding to the PCM with a low melting temperature and out from the tubes corresponding to the PCM with a high melting temperature during the charging process. The initial temperature field of each phase change heat storage device was set at 367K. The inlet temperature of the heat transfer fluid was set at 310K, and the inlet velocity was 0.2 m/s.

ANSYS software was used to solve and calculate the above models. A realizable k- ε turbulence model was adopted in the fluid part, and the Solidification/melting model was adopted in the phase transition process. The heat transfer fluid outlet in each phase change heat storage device is set as the free flow boundary condition. Coupling boundary conditions are set for the contact walls between the heat transfer fluid and the phase change materials and between different phase change materials.

Table 3. The initial and boundary conditions of the simulation

Type		Mathematical model	Definition
Boundary conditions	Tube	$T_f(x=0,t)=T_{inlet}$	T_{inlet} inlet temperature of the HTF
		$v_{in,x}(x=0,t)=v_{inlet}$	v_{inlet} inlet velocity of the HTF
		$v_{in,y}(x=0,t)=0$	$v_{in,x}$ velocity of the x-direction of the HTF
		$\left.\frac{\partial T}{\partial y}\right\|_{y=0}=0$	$v_{in,y}$ velocity of the y-direction of the HTF
	Shell	$\left.\frac{\partial T}{\partial y}\right\|_{y=50}=0$	

	Interface	$k\left.\frac{\partial T}{\partial y}\right\|_{y=5} = \lambda(T - T_{PCM})$	
Initial conditions		$T\ (x, y, t = 0) = T_0$	T_0 initial temperature

2.4 Numerical validation

It is used ICEM CFD to divide the structural grid of the cascade heat storage system, and the heat transfer boundary was encrypted. In order to test the grid independence of the solution, the different numbers of grids were obtained respectively. The melting fraction of heat storage material when the velocity of HTF is 0.5m/s was taken as the basis for grid independence verification. The simulation results of this model under different grid numbers as shown in Fig. 4. The mesh of 32415 elements was found to be optimum for the present study.

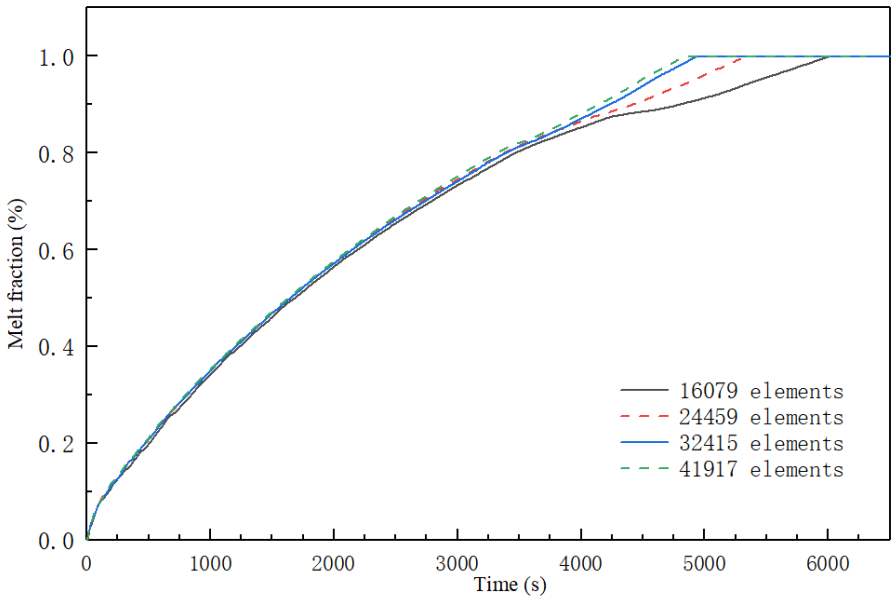

Fig.4. Grid independence verification

Then the Time step independence verification has been done. Based on the mesh elements set as 32415, the simulation was carried out with the time step of 0.5 seconds, 1.0 seconds, 1.5 seconds and 2.0 seconds. The time step was verified independently, and the verification method was similar to the grid independence verification. The influence of the time step on temperature simulation results is shown in Fig. 5. The simulation results show that when the time step is set to 1.0 seconds and 1.5 seconds, the temperature of the selected point has no significant difference. Therefore, selecting 1.0 seconds as the time step in the solution process of the model can achieve both accuracy and efficiency.

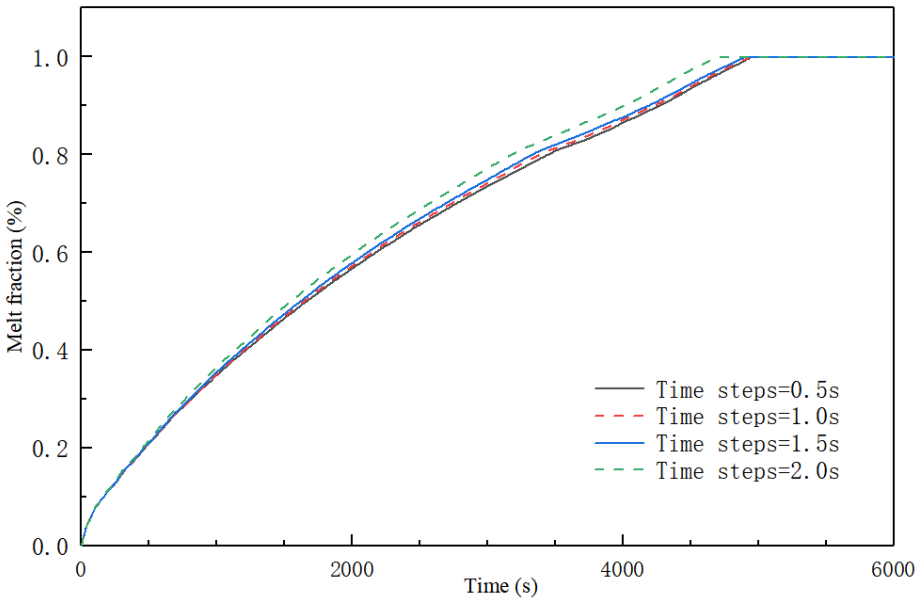

Fig.5. Time Step Independent Verification

To verify the reliability of the model, complete validation has been done to compare with the results of the real experimental of Akgün et al.[38] . All heat transfer processes and associated conditions in their experiment have been simulated. The present model is used to simulate the temperature of PCM in the double pipe heat storage device like this study, and the PCM temperature curve of the T_{11} in this experiment was compared and verified. Fig. 6-1 and Fig. 6-2 shows the results of two studies. It can be seen that there are little differences between the experimental results and the simulation results, and the difference between the two results remained within 10 %. It proves the authenticity of this numerical model. Based on this, it shows that the assumptions involved in the current model are reliable, and it can be used for subsequent simulation research.

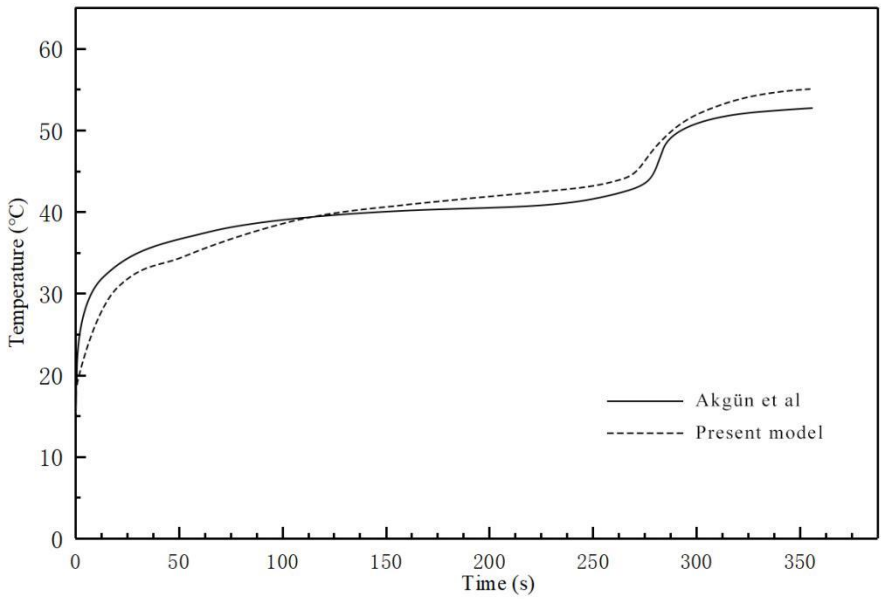

Fig.6-1.Validation with results of Akgün et al.

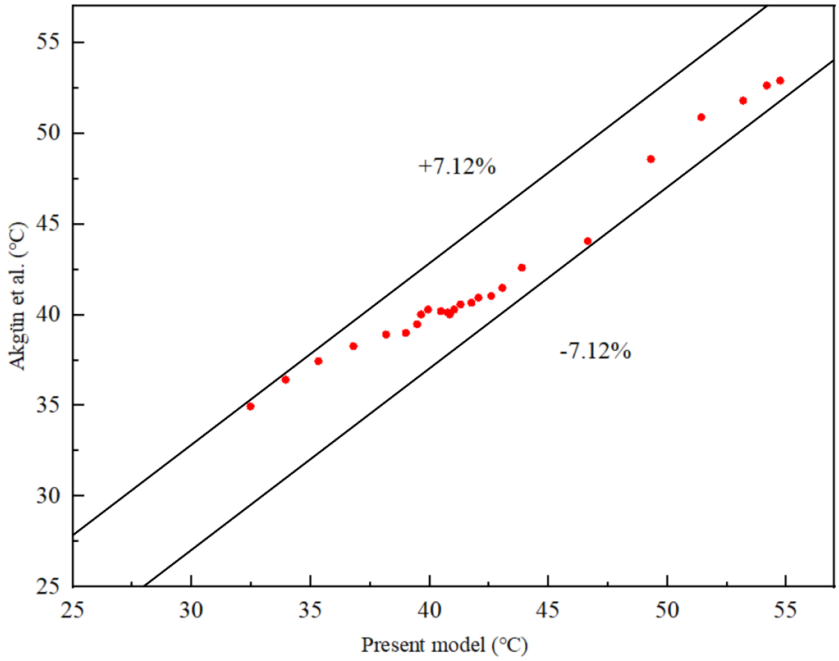

Fig.6-2.Validation with results of Akgün et al.

2.5 Evaluation index of LHTESS

Heat storage capacity, charging and discharging efficiency, melt fraction, and heat flux of charging and discharging are used as indexes in this paper to assess the charging and discharging performance of the LHTESS. The cumulative heat contained in LHTESS from the start of heat storage to a certain point in time is referred to as heat storage capability. Assuming that the outer shell of the heat accumulator is adiabatic and the heat loss of the heat accumulator is ignored. The melt fraction refers to the proportion of phase change material in the phase change heat storage device.

The heat flux of charging and discharging refers to the heat stored or released per unit time of LHTESS. It is usually calculated from the heat transfer on the heat transfer fluid side through the heat balance relationship. This index reflects the rate of charging and discharging heat in the heat accumulator. The outer wall of the heat accumulator is treated with insulation, and the heat loss of the heat accumulator is ignored. And the thermal recovery efficiency is the ratio of the accumulator's absorption enthalpy to the system's input enthalpy. The mathematical formulae and the meaning of the symbols of these indexes are shown in Table 4.

Table 4. The evaluation index

Evaluation index	Mathematical formula	Definition
Heat storage capacity	$Q_{max}=\sum_{j=1}^{n}Q_{ss,j}+Q_{l,j}+Q_{sl,j}$ $Q_{ss,j}=m_j c_{s,j}(T_{m,j}-T_0)$ $Q_{sl,j}=m_j c_{l,j}(T_j-T_{m,j})$ $Q_{l,j}=m_j h_j$	$Q_{ss,j}$ solid sensible heat of grade j PCM $Q_{sl,j}$ liquid sensible heat of grade j PCM $Q_{l,j}$ latent heat of grade j PCM Q_{max} theoretical maximum heat storage of the cascade system
Melt fraction	$\beta=\begin{cases}0 & T_p<T_s\\ \frac{(T_p-T_s)}{(T_l-T_s)} & T_s<T_p<T_l\\ 1 & T_l<T_p\end{cases}$	T_s solidification temperature of the PCM T_l melting temperature of the PCM T_p temperature of the PCM β melt fraction of the PCM

Heat flux	$q_i = \rho_l q_l c_l \Delta T_i$	ρ_l density of the HTF q_l inlet volume flow of the HTF c_l specific heat of the HTF ΔT_i temperature difference between inlet and outlet of the HTF q_i heat flux of the HTF
Thermal recovery efficiency	$\eta = \frac{H_{in} - H_{out}}{H_{in}} = \frac{H^t_{pcm} - H^0_{pcm}}{H_{in}}$	H_{in} enthalpy of the HTF at the inlet H_{out} enthalpy of the HTF at the outlet H^t_{pcm} enthalpy of the PCM at the time t H^0_{pcm} enthalpy of the PCM at the initial time η thermal recovery efficiency of the system

3. Results and discussion

3.1 Charging process of thermal storagy system

In the charging stage, the initial temperature field of four different PCM was set at 310 K, the inlet velocity of HTF was 0.2 m/s, and the inlet temperature was 367 K. The heat storage capacity, melt fraction, heat flux, and thermal recovery efficiency of different PCM was compared.

3.1.1 Heat storage capacity

The heat storage of different PCM filling schemes calculated according to Table 4 is shown in Table 5.

Table 5. Heat storage of different phase change materials arrangement

	Q_{ss}(kJ)	Q_l(kJ)	Q_{sl}(kJ)	Heat storage(kJ)
Cascade system	550.06	1557.02	385.18	2492.26
Single stage binary material	801.16	2129.35	275.87	3206.38
Single stage 60# paraffin	455.42	1206.49	536.24	2198.15
Single stage stearic acid	393.6	1335.23	343.41	2072.24
water	-	-	1667.18	1667.18

It can be seen from the calculation that the theoretical maximum heat storage of the cascade phase change accumulator is 2492.26 kJ, of which the latent heat of PCM accounts for 62.47%. At the same volume and working temperature, the theoretical maximum heat storage of the cascade PCM is 16.85% and 11.80% higher than the single-stage PCM using single-stage stearic acid and 60# paraffin, and 33.11% higher than the water as the heat storage medium.

The theoretical maximum heat storage of single-stage and cascade heat storage system is obtained by simulation, as shown in Fig. 7.

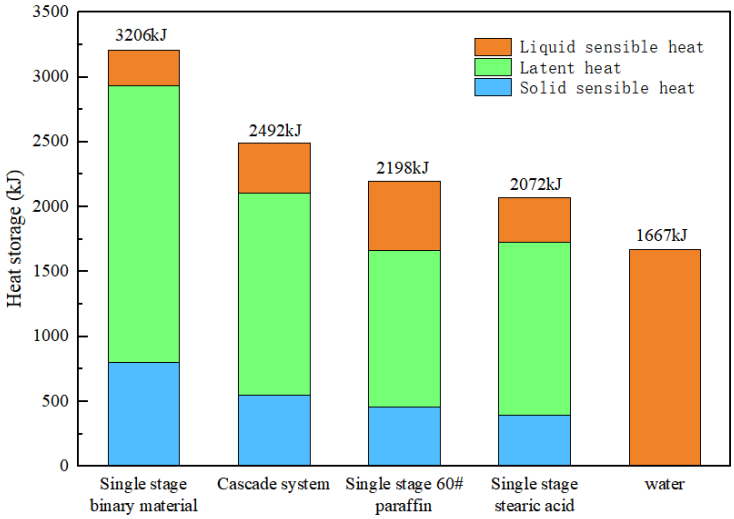

Fig.7. Maximum heat storage of different latent heat storage system

3.1.2 Melt fraction

The melt fraction-time variation curve of the cascade system and the single-stage system during the charging process is shown in Fig.8.

It can be found that the time required for the melt fraction to reach 1 is almost the same for the single-stage heat accumulator using binary PCM and 60# paraffin. The reason of the binary phase change materials melting fast is that $MgSO_4 \cdot 7H_2O$-$KAl(SO_4)_2 \cdot 12H_2O$ modified by EG has a more significant thermal conductivity and a minor specific heat in the solid phase, thus achieving a faster heating rate and shorting phase transition time. And the reason of the 60# paraffin melts fast is that it has medium thermal conductivity and small latent heat of phase transformation. Due to its small latent heat of phase change, it does not need much heat to reach the complete melting state, and thus has nearly the same melting efficiency as binary phase change materials. But its heat storage capacity is not as good as binary phase change materials.

Cascade system takes 7040s for the PCM melt fraction to reach 1. Although the cascade system is used, it does not show a significant advantage in the melting efficiency. The main reason is that the cascade system needs to wait for the slowest stage to melt completely. Compared with single stage stearic acid, the melting efficiency of stearic acid in cascade system has been significantly improved.

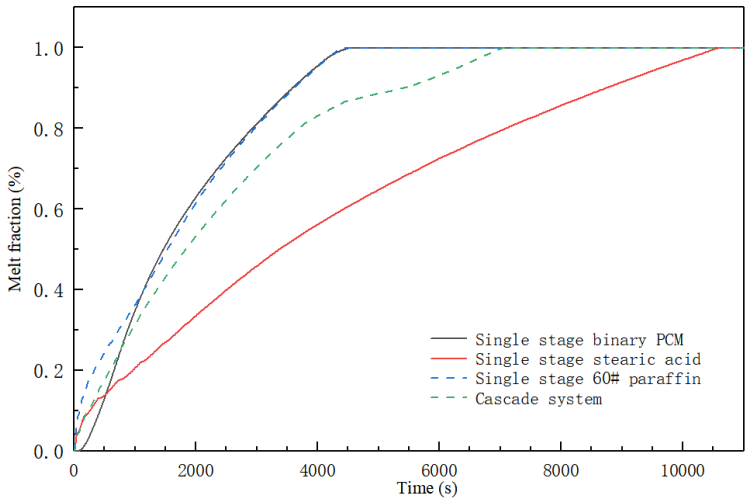

Fig.8. Variation curve of melt fraction of cascade system with different PCM

In the process of charging, the melt fraction and time variation curve of PCM in each region of the cascade

system is shown in Fig.9.

In the cascade system, the total melting time of three different regions during the charging process is 4500s, 7048s, and 4450s, respectively. Unlike the single stage heat accumulator, at about 3760 seconds, the melting efficiency of binary PCM region slows down significantly. And at about 5660 seconds, the melting rate of stearic acid region begins to accelerate significantly.

The reason for this phenomenon is that coupling boundary conditions are used at the boundary surfaces of the two regions. Binary PCM has the most considerable thermal conductivity, and the melting temperature of stearic acid is lower than that of binary PCM. Thus, at the junction of the two materials, a large amount of heat is transferred from the binary PCM area to the stearic acid area. In addition, after the 60# paraffin has completely melted, it begins to absorb sensible heat and thus the temperature continues to rise, and higher than that of the stearic acid region. Therefore, heat transfer from the 60# paraffin region and the binary PCM region to the stearic acid region. So the melting rate of stearic acid began to increase significantly after 5660 seconds.

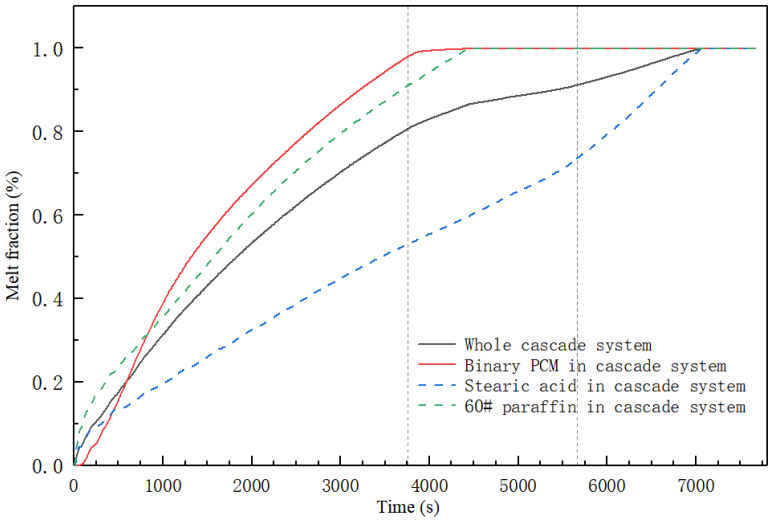

Fig.9. Variation curve of melt fraction of PCM in different regions in LHTESS

The melt fraction-time variation curve of PCM in the middle region of different accumulators is shown in Fig.10.

It can be found that the single-stage accumulator using stearic acid takes 10608s to reach the melt fraction to 1. And the melt fraction of the stearic acid in the cascade system takes 7048s to reach 1, which is 33.36% shorter than a single stage accumulator. It is shown that the time required for the complete melting of PCM in the intermediate region can be significantly shortened under the action of PCM in the adjacent region in the cascade phase change heat storage.

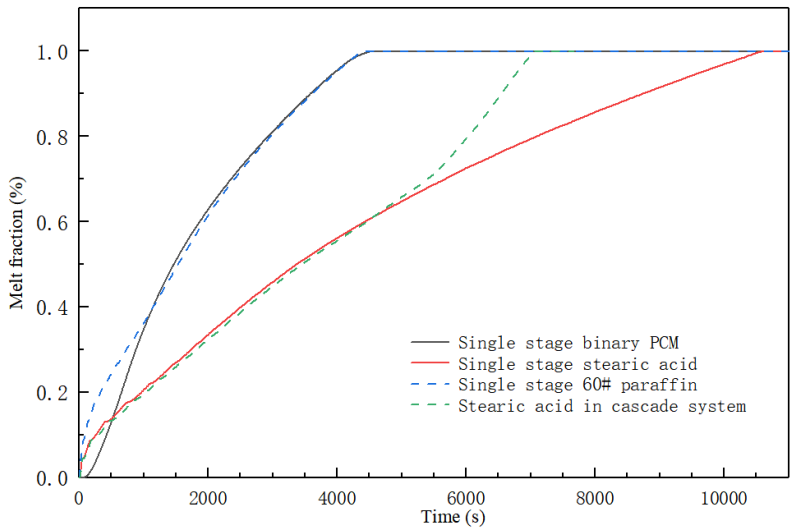

Fig.10. Variation curve of melt fraction of PCM in the middle region of different LHTESS

3.1.3 Heat flux

In the charging process of the accumulator with different PCM filling schemes, the overall heat flux at the heat exchange wall is shown in Fig.11.

The main factors affecting the heat flux are the thermal resistance and heat transfer temperature difference. During the process of charging, the temperature in the PCM area increases gradually, and the heat flux on the wall of the heat transfer fluid pipeline decreases gradually. Because the thermal conductivity of binary PCM is much higher than that of stearic acid and 60# paraffin, the wall heat flux of the single-stage PCM is higher than that of the other two single-stage PCM. However, with the increase of temperature in the PCM area, the heat flux of the binary PCM also decreases rapidly. After the 4528s, the binary PCM is completely melted, and the heat flux of the binary PCM gradually decreases to the level below the single stage stearic acid heat accumulator and the single stage 60# paraffin heat accumulator.

Compared with the single stage stearic acid heat accumulator and the single stage 60# paraffin heat accumulator , the heat flux of the cascade PCM is more higher, and the curve is relatively stable. This is mainly because the heat transfer temperature difference is more stable in the cascade PCM system. Therefore, during the charging process of the cascade PCM accumulator, the heat flux on the wall of the HTF pipeline can be stable and maintained at a relatively high level.

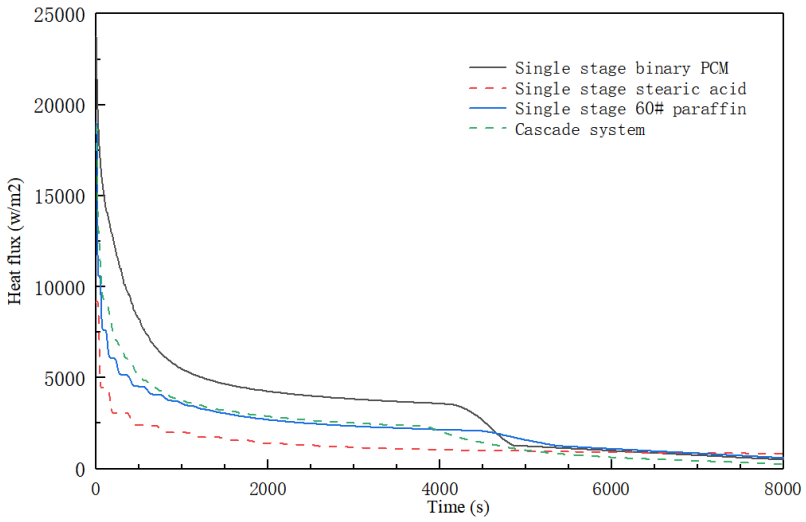

Fig.11. Heat Flux of Pipe Surfaces of Different Latent Heat Storage System

3.1.4 Thermal recovery efficiency

The thermal recovery efficiency of the heat accumulator in the charging process using different phase change materials was calculated, and the results are shown in Fig.12.

It can be found from the simulation results that the thermal recovery efficiency of the cascade PCM accumulator reaches 61.57%, which is slightly lower than that of the single-stage PCM system using 60# paraffin. And the thermal recovery efficiency of the cascade system was 18.42% and 10.06% higher than that of the single-stage system using the other two PCMs.

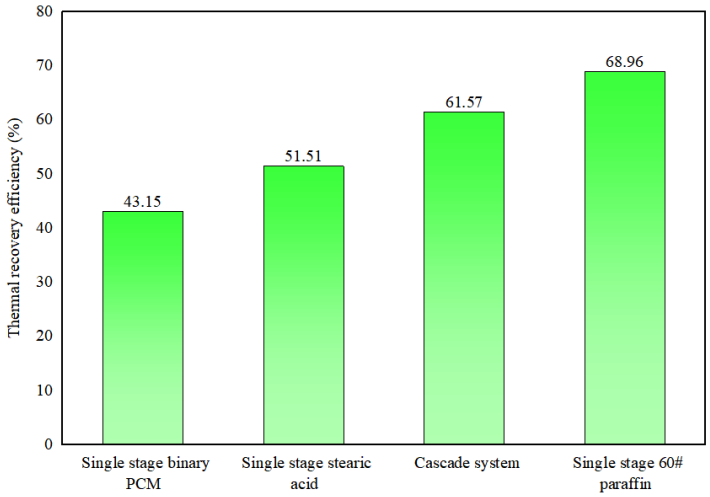

Fig.12. Thermal Recovery Efficiency of Different Latent Heat Storage System

3.2 Discharging process of thermal storagy system

In the discharging process, the initial temperature field of four different PCM filling schemes was set at 367 K, the inlet velocity of HTF was 0.2 m/s, and the inlet temperature was 310 K. The HTF enters through the pipeline corresponding to the 60# paraffin location and leaves from the pipeline corresponding to the binary PCM location. The melt fraction and heat flux of different phase change material filling schemes were compared, respectively.

3.2.1 Melt fraction

The melt fraction-time variation curve of the cascade system and the single-stage accumulator during the discharging process was shown in Fig.13.

According to the simulation results, in the single-stage accumulator, using binary PCM releases heat faster in the solidification process, and the complete solidification time of the material was 1608s. The total solidification time of the PCM in the accumulator using stearic acid and 60# paraffin was 7600s and 5920s, respectively. This is mainly because the thermal conductivity of EG-$MgSO_4 \cdot 7H_2O$-$KAl(SO_4)_2 \cdot 12H_2O$ composite PCM is significantly improved under the action of EG, so melting and solidification are more rapid.

Similar to the charging process, the cascade LHTESS needs to wait for the stearic acid discharging complete, so the discharging efficiency is not high. However, compared with single stearic acid stage, the discharging efficiency of stearic acid stage in cascade system has been significantly improved.

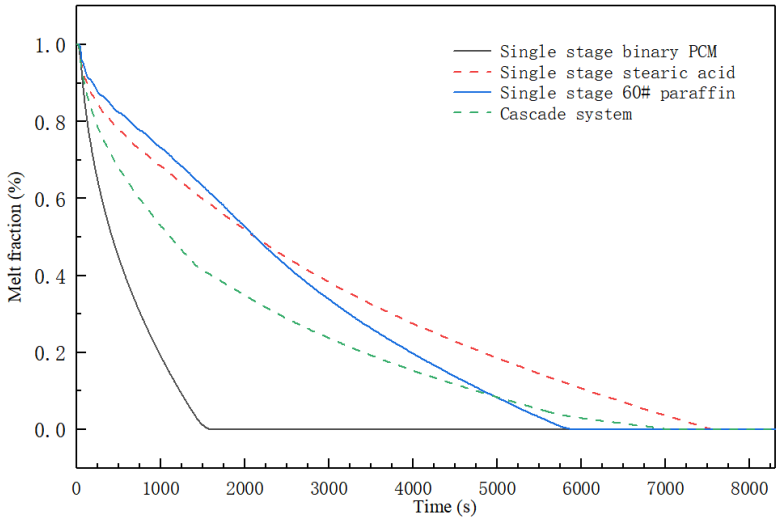

Fig.13. Variation curve of melt fraction of cascade system with different PCM

In the cascade LHTESS, the melt fraction-time curves of different regions are shown in Fig.14. It can be found that although the binary PCM region is farthest from the entrance of HTF, due to its maximum thermal conductivity and slight temperature difference between its melting temperature and the initial temperature, the melt fraction of PCM in this region drops fastest, solidifies first and solidifies completely first, and the solidification time is 1440s. The PCM in the other two regions solidified completely almost simultaneously, which took 7060s and 6610s, respectively.

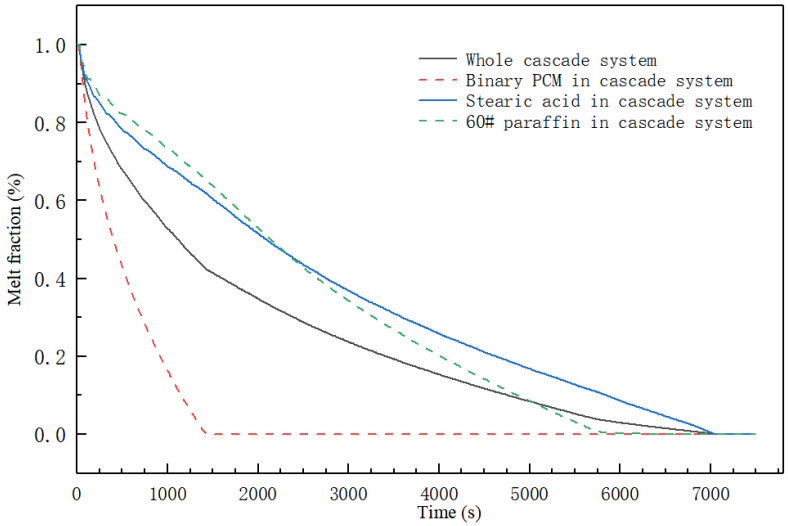

Fig.14. Variation curve of melt fraction of PCM in different regions in LHTESS

3.2.2 Heat flux

In the discharging process of the accumulator with different PCM filling schemes, the overall heat flux of the wall surface is shown in Fig.15. Since the heat flux of each wall is negative during discharging, the absolute values of all the heat flux results are taken for the convenience of comparison.

According to the simulation results, with the process of discharging, the heat flux on the wall of the accumulator decreases gradually. This is mainly due to the gradual decrease in temperature in the phase change material region. For the single-stage system, the heat flux of the single-stage material filled with binary PCM is higher than that filled with stearic acid and 60# paraffin, mainly because of the thermal conductivity of EG-$MgSO_4 \cdot 7H_2O$-$KAl(SO_4)_2 \cdot 12H_2O$ is much higher than that of the other two PCM. However, the temperature of binary PCM drops faster,

and the time of complete discharge is shorter. Therefore, after the complete discharge of binary PCM, the temperature difference between the heat accumulator and the HTF is more low. As a result, after 2300s, the wall heat flux is lower than that of LHTESS of the other two PCM.

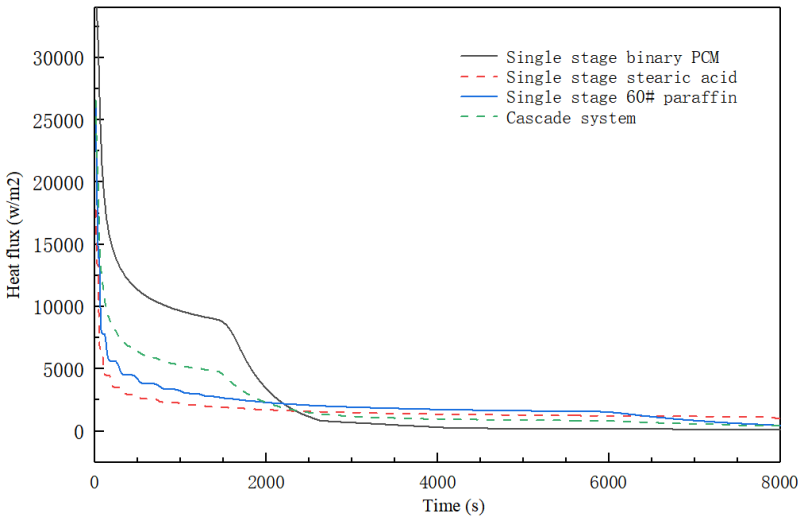

Fig.15. Heat Flux of Pipe Surfaces of Different Latent Heat Storage System

As can be seen from the above results, the heat charging and heat discharging efficiency of the PCM with the low heat charging and discharging efficiency in the system greatly affects the overall efficiency of the system. However, in practical engineering applications, it is not necessary to completely charge and discharge all PCM in the system. In fact, the overall phase transformation fraction of the system reaches 80% is acceptable. Therefore, considering the acceptable range of phase transformation fraction reaching 80%, LHTESS has certain advantages in terms of heat transfer efficiency and heat flow density. It is due to its advantages of uniform heat exchange temperature difference and high internal heat transfer between different PCM. Therefore, if complete phase transformation of PCM is not required, and 80% phase transformation fraction is taken as an acceptable range, LHTESS can improve multiple performance compared with the traditional system.

3.3 Influence of the HTF flow state on the C-LHTESS performance

The diameter of the HTF pipeline of the cascade heat storage system is 10mm, the critical Reynolds number is 2000-2600, and the critical velocity can be calculated as 0.202-0.262m/s. To explore the effect of the Reynolds number of the different HTF on the performance of the cascade heat storage system, the velocity at the entrance of HTF was set as 0.1, 0.2, 0.5, 1.0 and 2.0 m/s in the charging process, and the Reynolds numbers are 995.2, 1990.4, 4976.1, 9952.1 and 19904.3, respectively. It can be seen that when the Reynolds number exceeds the critical Reynolds number at flow rates of 0.5, 1.0 and 2.0 m /s, the flow state can be considered as sufficiently turbulent. And when the flow rates are 0.1 and 0.2m/s, the Reynolds number is lower than the critical Reynolds number, and the laminar flow is the main flow state. The initial temperature field is set at 310 K, and the HTF inlet temperature is set at 367 K.

The melt fraction-time curve of the cascade heat storage system with different Reynolds number of the HTF is shown in Fig.16, and the time required for complete melting of the phase change material is shown in Fig.17.

The heat storage total time of the cascade latent heat storage system decreases with the increase of the heat transfer fluid's Reynolds numbers. When the Reynolds numbers are 995.2, 1990.4, 4976.1, 9952.1 and 19904.3, the heat storage time of the cascade heat storage device is 8968s, 7048s, 4936s, 3112s and 1720s, respectively. It can be seen that in the cascade heat storage system, the heat storage completely time decreases significantly with the

increase of the Reynolds number of the HTF. In practical applications, the solar water heating system is often used to provide heat for such heat storage system, and the water pump provides kinetic energy for the HTF circulation. Therefore, in practical applications, it is necessary to consider the local solar heating capacity and the energy consumption of the pump. When the Reynolds number of HTF in this system reaches 19904.3, although the heat storage time of the system is greatly reduced, more energy of the pump is consumed at the same time, which is not economical and energy conservation. Therefore, it can be seen that when the Reynolds number in the system is close to 2000, The HTF is in laminar flow, it can meet the requirements of use under the condition of energy conservation.

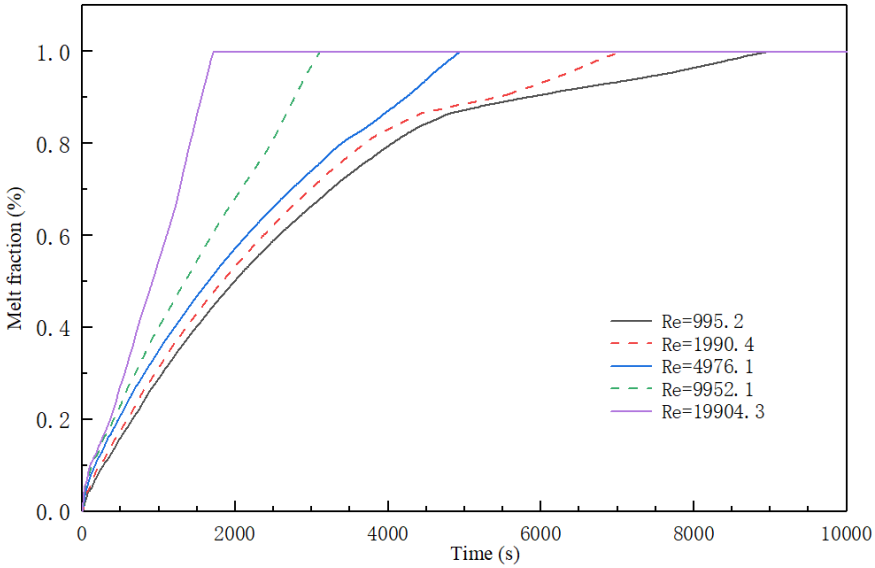

Fig.16. The curve of melt fraction of cascade latent heat storage system at different flow rates

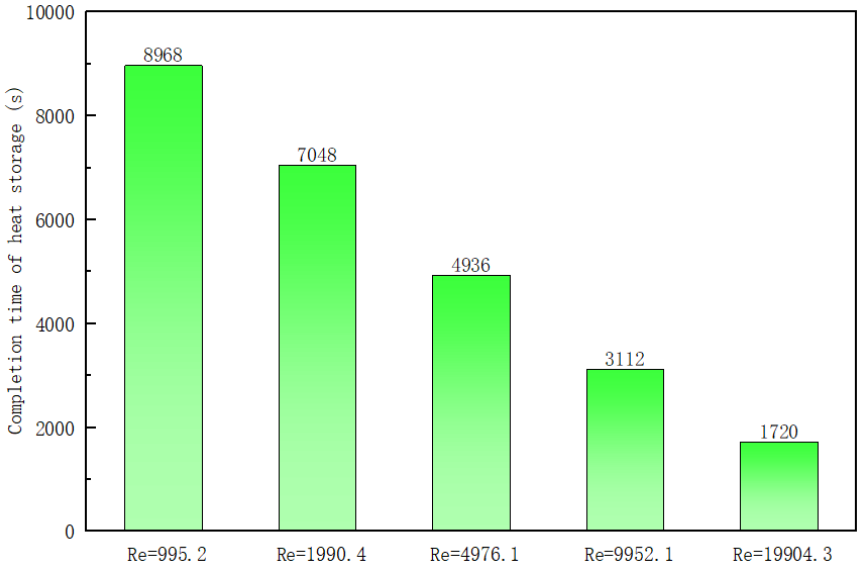

Fig.17. Melting time of cascade latent Heat storage system at a different velocity

3.4 Advantages

As can be seen from the above results, it is feasible to optimize the original heat storage equipment by using the C-LHTESS made of non-toxic phase change materials.This system has more advantages than traditional LHTESS in engineering application because of its constant temperature difference and harmless to human body.

Yan et al.[39] studied the use of PCM for the thermal management of wasted energy from a stand-alone hybrid

solar-wind-battery power system. They chose Ba(OH)2 • 8H2O as the PCM in the system because of its high heat storage capacity, but it has certain harm to human body. In our study, MgSO4 • 7H2O-KAl(SO4)2 • 12H2O binary mixed PCM was developed to replace Ba(OH)2 • 8H2O, which can not only obtain similar thermal physical properties, but also reduce the harm to human body. It is also feasible to use binary mixed materials instead of Ba(OH)2 • 8H2O in other system, which can meet the requirements of the system and reduces toxicity. However, the properties of non-toxic binary PCMs are not completely superior to Ba(OH)2 • 8H2O. The latent heat of Ba(OH)2 • 8H2O is 280kJ/kg, while that of binary PCMs is 175.8kJ/kg, which is smaller than that of Ba(OH)2 • 8H2O. However, the thermal conductivity of non-toxic binary PCMs is much higher than that of Ba(OH)2 • 8H2O, and the defect of low latent heat can be reduced by using C-LHTESS. Therefore, the performance of C-LHTESS with non-toxic materials maybe is better.

Yang et al.[40] investigates methods for selecting PCM based on the required conditions. In their specific case, Ba(OH)2 • 8H2O was selected as the optimal PCM for heat storage in a ground source heat pump system based on the algorithm. Similarly, due to the toxicity of Ba(OH)2 • 8H2O, it may cause certain harm to personnel during installation and construction.Therefore, using mixed PCM with similar physical properties instead of Ba(OH)2 •8H2O can effectively solve this problem.The system can also be further optimized using C-LHTESS to enhance the heat transfer capability, the system mentioned in this study can be directly used to modify the original system. However, this will increase the system complexity and equipment cost. Therefore, one of the factors in the choice of system depends on the requirements of the project.

Jyoti et al.[41] designed a solar thermal water heating system using a custom-built latent heat storage tank with different PCMs. In their research, they used variety of PCMS to collect solar energy, all of them were non-toxic. In their study, they chose a single-stage LHTESS for heat storage. In fact, with these different materials, the efficiency of the system could be improved by non-toxic C-LHTESS using the structure of the device described in our study. Therefore, the study of non-toxic C-LHTESS has great engineering significance and can be used to further optimize the existing heat storage system. However, the disadvantage of such optimization is that the complexity and stability of the system are not as high as that of the traditional system, which requires further experimental verification in different scenarios.

Therefore, the following two aspects need to be further discussed in future studies:

On the premise of maintaining non-toxicity and high thermal conductivity of PCM, improve its heat storage capacity and reduce production cost;

In different scenarios, the applicability and stability of the equipment are studied experimentally, and the heat storage equipment suitable for different application scenarios will be developed.

4. Conclusions

?MgSO4-KAl(SO4)2, stearic acid, and 60# paraffin were screened as PCMs for C-LHTESS and their thermal performances were studied.. A mathematical model was established to simulate its heat charging and heat discharging process. The heat storage capacity, melt fraction, heat flux, and thermal recovery efficiency of the cascade and the single-stage latent heat storage system were analyzed. The influence of Reynolds number of HTF on the heat storage total time of the cascade latent heat storage system was investigated. The research conclusions were listed as follows:

(1) In order to improve the heat charging and discharging performance of the heat storage system with fixed PCM, C-LHTESS concept is applicable.

(2) Under the same constrcution parameters and operation conditions, the heat storage capacity of the C-LHTESS is higher than that of the single-stage stearic acid and single-stage 60# paraffin system. Further, the capacity is 33.11% higher than that with water as the heat storage medium. The thermal recovery efficiency of the cascade latent heat storage system is 61.6%, which is higher than that of the single-stage MgSO4 • 7H2O-KAl

(SO4)2 • 12H2O binary PCM heat storage system and the single-stage stearic acid latent heat storage system.

(3) The thermal conductivity of PCM has a significant effect on the heat transfer performance of each system. The heat charging and heat discharging time of the C-LHTESS is less than the single-stage stearic acid latent heat storage system. And higher than that of the single-stage 60# paraffin and the single-stage MgSO4 • 7H2O-KAl(SO4)2 • 12H2O binary PCM latent heat storage system.

(4) In the process of charging and discharging, the average heat flux of the C-LHTESS is only lower than the single-stage MgSO4 • 7H2O-KAl (SO4)2 • 12H2O binary PCM system with very high thermal conductivity. Compared with the other single-stage heat storage system, its heat flux is more higher.

(5) The heat storage time of the C-LHTESS decreases with the increase of the Reynolds number. But consider the practical applications, high Reynolds number results in high pump consumption. From the perspective of reducing energy consumption, it is recommended that the Reynolds number of the heat transfer fluid is about 2000 and the flow state is laminar.

Nomenclature

Symbols

c	specific heat, J/kg K
h	enthalpy, J/kg
H	total enthalpy, J/kg
k	thermal conductivity, W m^{-1} K^{-1}
q	volume flow, m^3/s
T	temperature, K
v	velocity, m/s
β	melt fraction
λ	thermal conductivity, W/m K
ρ	density, kg/m^3
μ	dynamic viscosity, Pa s
η	thermal recovery efficiency
Δ	difference

Subscripts

0	initial
f	heat transfer flow
i	grade i
j	grade j
l	liquid phase
m	melting
max	maximum
r	reference
s	solid phase
sl	liquid sensible heat
ss	solid sensible heat
x	x direction
y	y direction
p	PCM

Abbreviations

PCM	phase chang material
HTF	heat transfer fluid
LHTESS	latent heat thermal energy storagy system
C-LHTESS	Cascade latent heat thermal energy storagy system

References:

1. Liobikienė G, Dagiliūtė R, Juknys R. The determinants of renewable energy usage intentions using theory of planned behaviour approach. RENEW ENERG. 2021;170:587-594.
2. Mrabet Z, Alsamara M, Saleh AS, Anwar S. Urbanization and non-renewable energy demand: A comparison of developed and emerging countries. ENERGY. 2019;170:832-839.
3. Li T, Li A, Guo X. The sustainable development-oriented development and utilization of renewable energy industry——A comprehensive analysis of MCDM methods. ENERGY. 2020;212:118694.
4. BP. BP Energy Outlook 2020 edition. London, UK2020. p.
5. Alizadeh M, Sadrameli SM. Numerical modeling and optimization of thermal comfort in building: Central

composite design and CFD simulation. ENERG BUILDINGS. 2018;164:187-202.

6. Kuznik F, Virgone J. Experimental investigation of wallboard containing phase change material: Data for validation of numerical modeling. ENERG BUILDINGS. 2009;41:561-570.

7. Shukla A, Kant K, Sharma A. Solar still with latent heat energy storage: A review. INNOV FOOD SCI EMERG. 2017;41:34-46.

8. Siddiqui O, Dincer I. Development of a sustainable energy system utilizing a new molten-salt based hybrid thermal energy storage and electrochemical energy conversion technique. Sustainable Energy Technologies and Assessments. 2020;42:100866.

9. Sunku Prasad J, Muthukumar P, Anandalakshmi R, Niyas H. Comparative study of phase change phenomenon in high temperature cascade latent heat energy storage system using conduction and conduction-convection models. SOL ENERGY. 2018;176:627-637.

10. Merlin K, Soto J, Delaunay D, Traonvouez L. Industrial waste heat recovery using an enhanced conductivity latent heat thermal energy storage. APPL ENERG. 2016;183:491-503.

11. Yousef MS, Hassan H. Energetic and exergetic performance assessment of the inclusion of phase change materials (PCM) in a solar distillation system. ENERG CONVERS MANAGE. 2019;179:349-361.

12. Alvaro DG, Luisa FC. Phase change materials and thermal energy storage for buildings. Energy & Buildings. 2015;103.

13. Lohrasbi S, Gorji-Bandpy M, Ganji DD. Thermal penetration depth enhancement in latent heat thermal energy storage system in the presence of heat pipe based on both charging and discharging processes. ENERG CONVERS MANAGE. 2017;148:646-667.

14. Zhang C, Zhang X, Qiu L, Zhao Y. Thermodynamic analysis and improvement of cascaded latent heat storage system using temperature-enthalpy diagram. ENERGY. 2021;219:119573.

15. Christopher S, Parham K, Mosaffa AH, Farid MM, Ma Z, Thakur AK, et al. A critical review on phase change material energy storage systems with cascaded configurations. J CLEAN PROD. 2021;283:124653.

16. Horst M, Robert P. Cascaded latent heat storage for parabolic trough solar power plants. SOL ENERGY. 2006;81.

17. Wang Jianfeng OYZS. EXPERIMENTAL STUDY ON CHARGING PROCESSES OF A CYLINDRICAL HEAT STORAGE CAPSULE EMPLOYING MULTIPLE PHASE CHANGE MATERIALS. Shanghai, China2000. p. 5.

18. S. J, Sanjay DP. Performance enhancement in latent heat thermal storage system: A review. Renewable and Sustainable Energy Reviews. 2009;13.

19. Christopher S, Parham K, Mosaffa AH, Farid MM, Ma Z, Thakur AK, et al. A critical review on phase change material energy storage systems with cascaded configurations. J CLEAN PROD. 2021;283:124653.

20. Solomon L, Oztekin A. Exergy analysis of cascaded encapsulated phase change material — High-temperature thermal energy storage systems. Journal of Energy Storage. 2016;8:12-26.

21. Hamidreza S, Christopher WR, Theodore LB, Amir F. Heat transfer and exergy analysis of cascaded latent heat storage with gravity-assisted heat pipes for concentrating solar power applications. SOL ENERGY. 2012;86.

22. Peiró G, Gasia J, Miró L, Cabeza LF. Experimental evaluation at pilot plant scale of multiple PCMs (cascaded) vs. single PCM configuration for thermal energy storage. RENEW ENERG. 2015;83:729-736.

23. Dzikevics M, Zandeckis A. Mathematical Model of Packed Bed Solar Thermal Energy Storage Simulation. Energy Procedia. 2015;72:95-102.

24. Yang L, Zhang X, Xu G. Thermal performance of a solar storage packed bed using spherical capsules filled with PCM having different melting points. ENERG BUILDINGS. 2014;68:639-646.

25. Bains PS, Singh H. Exploratory investigation of a new thermal energy storage system with different phase change materials having distinct melting temperatures. Journal of Energy Storage. 2018;19:1-9.

26. Taha KA, Muhammad MR. Latent Heat Energy Storage System with Continuously Varying Melting

Temperature. International Journal of Mechanical Engineering and Robotics Research. 2018;7.

27. Chandel SS, Agarwal T. Review of current state of research on energy storage, toxicity, health hazards and commercialization of phase changing materials. RENEW SUST ENERG REV. 2017;67:581-596.

28. Guo F, Li Y, Xu Z, Qin J, Long L. Multi-objective optimization of multi-energy heating systems based on solar, natural gas, and air- energy. Sustainable Energy Technologies and Assessments. 2021;47:101394.

29. Wang Q, Wang J, Chen Y, Zhao CY. Experimental investigation of barium hydroxide octahydrate as latent heat storage materials. SOL ENERGY. 2019;177:99-107.

30. Li X, Wei H, Lin X, Xie X. Preparation of stearic acid/modified expanded vermiculite composite phase change material with simultaneously enhanced thermal conductivity and latent heat. SOL ENERG MAT SOL C. 2016;155:9-13.

31. Madadi Avargani V, Norton B, Rahimi A, Karimi H. Integrating paraffin phase change material in the storage tank of a solar water heater to maintain a consistent hot water output temperature. Sustainable Energy Technologies and Assessments. 2021;47:101350.

32. Chriaa I, Karkri M, Trigui A, Jedidi I, Abdelmouleh M, Boudaya C. The performances of expanded graphite on the phase change materials composites for thermal energy storage. POLYMER. 2021;212:123128.

33. Yazici MY, Saglam M, Aydin O, Avci M. Thermal Energy Storage Performance Of PCM/Graphite Matrix Composite In A Tube-In-Shell Geometry. Thermal Science and Engineering Progress. 2021:100915.

34. Hussam J, Alina Ż, Navid K, Darem A, Tom L. Latent thermal energy storage technologies and applications: A review. International Journal of Thermofluids. 2020;5-6.

35. Anica T. An experimental and numerical investigation of heat transfer during technical grade paraffin melting and solidification in a shell-and-tube latent thermal energy storage unit. SOL ENERGY. 2005;79.

36. Ioan S, Alexandru D. Review on heat transfer analysis in thermal energy storage using latent heat storage systems and phase change materials. INT J ENERG RES. 2019;43.

37. Kalapala L, Devanuri JK. Parametric investigation to assess the melt fraction and melting time for a latent heat storage material based vertical shell and tube heat exchanger. SOL ENERGY. 2019;193:360-371.

38. Akgün M, Aydın O, Kaygusuz K. Experimental study on melting/solidification characteristics of a paraffin as PCM. ENERG CONVERS MANAGE. 2007;48:669-678.

39. Yan J, Lu L, Ma T, Zhou Y, Zhao CY. Thermal management of the waste energy of a stand-alone hybrid PV-wind-battery power system in Hong Kong. ENERG CONVERS MANAGE. 2020;203:112261.

40. Yang K, Zhu N, Chang C, Wang D, Yang S, Ma S. A methodological concept for phase change material selection based on multi-criteria decision making (MCDM): A case study. ENERGY. 2018;165:1085-1096.

41. Prakash J, Roan D, Tauqir W, Nazir H, Ali M, Kannan A. Off-grid solar thermal water heating system using phase-change materials: design, integration and real environment investigation. APPL ENERG. 2019;240:73-83.